Supporting Information

The Effect of Tin Doping on α-Fe_2O_3 Photoanodes for Water Splitting

Christopher D. Bohn[1†], Amit K. Agrawal[1,2], Erich C. Walter[1,3], Mark D. Vaudin[4], Andrew A. Herzing[5], Paul M. Haney[1], A. Alec Talin[1], Veronika A. Szalai[1†]

[1] Center for Nanoscale Science and Technology, National Institute of Standards and Technology, Gaithersburg, Maryland, 20899, USA.

[2] Dept. of Electrical Engineering and Computer Science, Syracuse University, Syracuse, NY, 13244, USA.

[3] Institute for Research in Electronics and Applied Physics (IREAP), University of Maryland, College Park, MD 20742, USA.

[4] Ceramics Division, National Institute of Standards and Technology, Gaithersburg, MD, 20899, USA.

[5] Surface and Microanalysis Science Division, National Institute of Standards and Technology, Gaithersburg, MD 20899, USA.

[†]Corresponding authors. Phone: 301-975-3792 (VAS), 301-975-4236 (CDB), Fax: 301-975-2303, Email: veronika.szalai@nist.gov, christopher.bohn@nist.gov

Synthesis details

For sputtered samples, depositions required a power of 200 W at 0.4 A to give 0.3 nm/s of α-Fe_2O_3 at room temperature with gas flowrates of O_2 (12 mL/min) and Ar (50 mL/min). The α-Fe_2O_3 film thickness was measured by profilometry and confirmed by SEM cross-section.

For hydrothermal samples, a solution of 0.15 mol/L iron chloride hexahydrate ($FeCl_3 \cdot 6H_2O$ mass fraction >99 %) and 1 mol/L sodium nitrate ($NaNO_3$ mass fraction >99 %) was brought to pH 1.5 by the addition of 1 mol/L hydrochloric acid. One FTO slide was placed conducting side up in a sealed glass container with 20 mL of solution and heated for 4 h at 95 °C,

and then immediately rinsed with deionized water. After preheating a muffle furnace, slides were placed in an air atmosphere for 2 h at 500 °C and promptly removed. The thickness of the resulting hydrothermal α-Fe_2O_3 was 300 nm ± 30 nm as determined by SEM. After permitting samples to cool to room temperature, further annealing was performed in some cases by preheating the furnace to 800 °C, inserting samples followed by rapid removal after 10 min.

A control sample was prepared by sputtering α-Fe_2O_3 with a thickness of 600 nm on 200 nm of Au with an adhesion layer of 20 nm Cr on float glass. This sample was annealed under the same conditions as the sputtered and hydrothermal samples but demonstrated no photocurrent, as shown in Fig. S1. Because annealing at 800 °C approached the melting temperature of the Au (1164 °C), a multimeter was used to measure the resistance of the Au layer before and after annealing to confirm that it remained conductive. Poisoning of the surface by evaporated Au can be ruled out because all slides were annealed together.

Two methods were attempted to determine the surface area of the samples. First monolayers of Orange II dye were deposited.[S1,S2] This method gave inconclusive results. The second method, krypton gas adsorption with diced samples, also returned inconclusive results. On the basis of the adsorption instrument's sensitivity, however, we estimate the roughness factor, defined as the real area divided by the geometric area, to be on the order of 20 or less for both the sputtered and hydrothermal samples that were annealed at 800 °C. In all calculations presented in the text, the geometric area was used for normalization.

Optical characterization

Figure S2 shows optical images of the sputtered and hydrothermal α-Fe_2O_3 samples at room temperature, after annealing at 500 °C for 2 h, and after annealing at 800 °C for a further 10 min.

The yellow FeOOH in the room temperature hydrothermal sample contrasts with the red α-Fe_2O_3 of the annealed samples. The samples are less transparent and become deeper red in color after heat treatment. Illumination from the back side demonstrates the non-uniform coverage of the hydrothermal sample.

An ultraviolet-visible spectrophotometer with a photodiode array equipped with tungsten and deuterium lamps was used to measure absorbance from 190 nm to 1100 nm in 1 nm increments. Figure S3 shows absorbance as a function of wavelength for the FTO substrate, hydrothermal and sputtered samples at room temperature, after heating at 500 °C for 2 h, and after further heating at 800 °C for 10 min. The shading indicates the standard deviation of 3 experiments. In all cases, the background absorbance at wavelengths larger than 600 nm increased with heating, which could be ascribed to roughening of the surface, observable by eye, causing increased scattering as well as to the deterioration of the FTO substrate. Considering that the samples annealed at 800 °C have a bandgap that is at most 0.2 eV below the 2.0 eV calculated for samples annealed at 500 °C suggests a difference in available photons for water splitting of at most 6 % between the samples. By contrast, the difference in photocurrent observed at 1.23 V *vs.* RHE is 3 orders of magnitude demonstrating that absorption alone is *not* sufficient to explain the change in photocurrent.

Non-uniform coverage is apparent in the hydrothermal samples as discontinuous absorbance: two strong absorbance lines corresponding to FTO and α-Fe_2O_3 are apparent and are indicated by the two down arrows in S3. Determination of the exact bandgap is difficult owing to the fitting procedure required in a Tauc analysis;[S3] nevertheless, the bandgap for the sputtered and hydrothermal samples at 800 °C can be estimated from the onset of absorbance to between 2.0 eV and 2.2 eV. A shift in absorbance towards longer wavelengths is observable for

both the sputtered and hydrothermal samples upon heat treatment suggesting that the bandgap decreases after heating. The incorporation of Sn dopants is the most likely cause of this decrease in bandgap.

X-ray characterization

X-ray diffraction was performed in air at room temperature with a copper source (Cu $K_{\alpha 1}$, λ = 0.15406 nm) at 40 kV and 30 mA. A step of 0.03° and dwell time of 4 s was used with 0.68° and 0.15° divergence and receiving slits, respectively. X-ray diffraction spectra for the synthesized samples annealed at different temperatures as well as for the FTO substrate are shown in Fig. S4. The presence of α-Fe_2O_3 (PDF 33-0664)[S4] is noticeable in the sputtered samples by peaks at 2θ of 35.61° and 63.99°, as indicated by the vertical lines in Fig. S4. The presence of these peaks and the absence of a maximum intensity peak at 24.14° suggest preferential orientation of the c-axis parallel to the substrate. The absence of peaks in the sputtered sample at 30.09° and 56.94°, 41.93°, and 44.67° was used to rule out the formation of Fe_3O_4 (PDF 19-0629), FeO (PDF 6-0615) and Fe (PDF 6-0696), respectively, during sputtering. Smaller peaks corresponding to α-Fe_2O_3 were observed in the hydrothermal samples compared to the sputtered samples after annealing, which could be explained by the smaller thickness and therefore smaller quantity of α-Fe_2O_3 material. For the hydrothermal sample at room temperature, the primary goethite (PDF 29-0713) peak at 21.22° is absent; however, a peak at 35.09° was observed, which may be attributed to akaganeite (PDF 42-1315).

Electron Microscopy Characterization

A focused-ion beam (FIB) instrument with a gallium source and primary beam voltage of 30 kV was used to prepare the 100 nm ± 20 nm thick α-Fe_2O_3 cross-sections; platinum was used as an overlayer and for attachment to the copper grids.

For energy dispersive X-ray spectroscopy (EDS), a primary beam of 10 kV and a 60 µm aperture were used. Calibration was performed with a silicon wafer (Si, K_α of 1.740 keV) and copper tape (Cu, K_α of 8.041 keV). A total of 2×10^7 counts were collected for each sample over 5 h. Sample drift was automatically corrected every 20 s and the maximum drift recorded was <35 nm. Simulations of X-ray generation in α-Fe_2O_3 were performed using NIST's Monte Carlo code DTSA-II (freeware).[S5] For α-Fe_2O_3 (PDF 33-0664) with density 5.26 g/cm^3, a primary beam voltage of 10 kV, the diameter of the X-ray generation volume with the beam perpendicular to the bulk material was determined to be ≈ 0.5 µm.

For scanning transmission electron microscopy (STEM) imaging, a primary beam acceleration of 300 kV was used with a post-column imaging energy-filter operating in spectroscopy mode for EELS acquisition. A 2.5 mm entrance aperture, 16 mrad illumination semiangle, 16 mrad collection semiangle, and energy dispersion of 0.5 eV/channel were used. Typically, 20 spectra were collected for approximately 0.7 s each over an area of 30 nm × 30 nm or at a single point. The spectra for the 500 °C sample were collected 200 nm from the FTO interface, while those for the 800 °C sample were collected at a distance of 70 nm but showed no noticeable variation with increasing distance from the interface.

For the EELS spectra, a power law background of the form:

$$f(\Delta E) = a\Delta E^{-b}, \quad \text{(S.1)}$$

where *a* and *b* are fitting parameters and ΔE is the energy loss, was subtracted using the windows 400 eV to 470 eV for Fig. 3(c) and 650 eV to 680 eV for Fig. 3(d). The intensity, *I*, of the Fe L_3 and L_2-edges was further calculated as follows. A background function of the form of Eq.(S.2) was subtracted:

$$f(\Delta E) = \frac{h_1}{\pi}\left\{\tan^{-1}\left[\frac{\pi}{w_1}(\Delta E - E_1)\right] + \frac{\pi}{2}\right\} + \frac{h_2}{\pi}\left\{\tan^{-1}\left[\frac{\pi}{w_2}(\Delta E - E_2)\right] + \frac{\pi}{2}\right\}, \quad \text{(S.2)}$$

where h_1,w_1, h_2 and w_2 are fitting parameters and $E_1 = 709$ eV and $E_2 = 721.5$ eV. This background function was fit over the intervals 650 eV to 700 eV and 730 eV to 780 eV and is shown in Fig. 3. Next, a Lorentzian function was fit over 650 eV to 780 eV to determine peak areas:

$$f(\Delta E) = \frac{h_1}{\pi}\left\{\frac{\frac{1}{2}w_1}{(\Delta E - E_1)^2 + \left(\frac{1}{2}w_1\right)^2}\right\} + \frac{h_2}{\pi}\left\{\frac{\frac{1}{2}w_2}{(\Delta E - E_2)^2 + \left(\frac{1}{2}w_2\right)^2}\right\}, \quad \text{(S.3)}$$

where h_1,w_1, h_2 and w_2 are unique fitting parameters and $E_1 = 709$ eV and $E_2 = 721.5$ eV as before. The ratio of $I(L_3)/I(L_2)$ was calculated using h_1/h_2 from Eq.(S.3) and gave 5.0 and 6.0 for the 500 °C and 800 °C sputtered samples, respectively, in agreement with published values of 4.7 to 6.5 for α-Fe_2O_3.[S6,S7]

SIMS characterization

The secondary ion was O_2^+; an accelerating potential of 8 kV and current of 100 nA was used; material was removed from a raster area of 150 µm × 150 µm. Distance was calculated by multiplying the instantaneous time of collection by the final crater depth, 1300 nm in in all cases, and dividing this product by the total acquisition time of approximately 22 min. This calculation assumes a linear sputtering rate, which our experimental data indicate is not entirely correct. For

600 nm thick hematite films, the interface was observed at 800 nm, using the distance calculation described above. To correctly recover the interface between α-Fe_2O_3 and FTO at 600 nm, the sputter rate in the α-Fe_2O_3 should be half that in the FTO. This difference is reasonable given the difference in chemical composition of the layers. The detection limit of the instrument based on a dynamic range of approximately six orders of magnitude was fixed at $10^{16}/cm^3$.

Solution to Poisson Equation

The Poisson equation is given by:

$$\nabla^2 V = \frac{-qN_d}{\epsilon\epsilon_0}. \tag{S.4}$$

Assuming a cylindrical geometry with a nanowire of radius, R, centered at $r = 0$ and a charge density which is uniform between r_0 and R and vanishes in the interior $(r < r_0)$, the potential difference between the interior and exterior of the wire is given by:

$$\left(V - V_{FB} - \frac{kT}{q}\right) + \frac{qN_d}{2\epsilon\epsilon_0}\left[\frac{(R^2 - r^2)}{2} + R^2 ln\left(\frac{r}{R}\right)\right] = 0, \tag{S.5}$$

where $R - r$ is the space charge width, V_{FB} is the flatband potential, T is the temperature, k is Boltzmann's constant, q is the elementary charge, N_d is the dopant density, ϵ is the relative permittivity of the semiconductor, ϵ_0 is permittivity of free space, r is the radius and $V(R) = V_{FB} + kT/q$.[S8] Considering the cylindrical structure of the α-Fe_2O_3 with radii of $R = 100$ nm in Figs. 1-3, most of the charge is contained in the cylinder's walls, $Q = qN_D\pi(R^2 - r^2)L$, over area $A = 2\pi RL$. The capacitance per unit area is then calculated using the expression for Q and Eq. (S.5) for V as:

$$C = \frac{1}{A}\frac{dQ}{dV} = \frac{2\epsilon\epsilon_0 r_0^2}{R(R^2 - r_0^2)}, \tag{S.6}$$

which leads to the Mott-Schottky expression for a cylinder,

$$\frac{1}{C^2} = \left[\frac{R(R^2 - r^2)}{2\epsilon\epsilon_0 r_0^2}\right]^2, \tag{S.7}$$

where r_0 is a function of V. For consistency with experimental results, however, the geometrical area must be used for normalization of the capacitance, and it is assumed that the geometrical area is one tenth the area of the cylinder side walls since for hexagonally closest packing, $\frac{\pi R^2}{0.91} \times \frac{1}{2\pi RL} \approx \frac{1}{10}$. This assumption also justifies ignoring surfaces perpendicular to the side walls in the calculation of capacitance and was used in plotting the curves in Fig. 4(f).

SI References:

(S1) Kay, A.; Cesar, I.; Grätzel, M. *J. Am. Chem. Soc.* **2006**, *128*, 15714-15721.
(S2) Bandara, J. ; Mielczarski, J. A.; Kiwi, J. *Langmuir* **1999**, *15*, 7670-7679.
(S3) Tauc, J.; Grigorovici, R.; Vancu, A. *Phys. Status Soidi* **1966**, *15*, 627-637.
(S4) PDF, Powder Diffraction File, produced by International Centre for Diffraction Data, 12 Campus Blvd., Newtown Square, PA. 19073-3273, USA.
(S5) Ritchie, N.W.M. *Microsc. Microanal.* **2009**, *15*, 454-468.
(S6) Colliex, C.; Manoubi, T.; Ortiz, C. *Phys. Rev. B* **1991**, *44*, 11402-11411.
(S7) van Aken, P. A.; Liebscher, B. *Phys. Chem. Miner.* **2002**, *29*, 188-200.
(S8) Mora-Seró, I.; Fabregat-Santiago, F.; Denier, B.; Bisquert, J.; Tena-Zaera, R.; Elias, J.; Lévy-Clément, C. *App. Phys. Lett.* **2011**, *89*, 203117.

Table S1. Four point probe measurements of sheet resistance of the FTO substrates gave (7.5 ± 0.3) Ω × m^2 / m^2 at room temperature, (6.9 ± 0.1) Ω × m^2 / m^2 after annealing at 500 °C for 2 h, and (11.4 ± 0.3) Ω × m^2 / m^2 after annealing at 800 °C for a further 10 min.

	RT	500°C	800°C
ρ (Ω×m^2/m^2)	7.5±0.3	6.9±0.1	11.4±0.3

Figure S1. Current density (*J*) *vs.* potential for α -Fe_2O_3 sputtered samples with a thickness of 600 nm on FTO, hydrothermal samples with a thickness of 300 nm on FTO and sputtered films with a thickness of 600 nm on 200 nm of Au, 20 nm of Cr and float glass. In all cases, samples were annealed at 500 °C for 2 h followed by 800 °C for 10 min. The electrolyte was 1 mol/L NaOH (pH 13.6); calibrated AM 1.5 light at 100 mW/cm^2 illuminated each sample; the scan rate was 10 mV/s. For the sample with Au as the back contact, no Sn doping with heat treatment is possible and no photocurrent is observed leading to the conclusion that doping is indeed necessary for photocurrent. Shading indicates a single standard deviation calculated from at least three experiments.

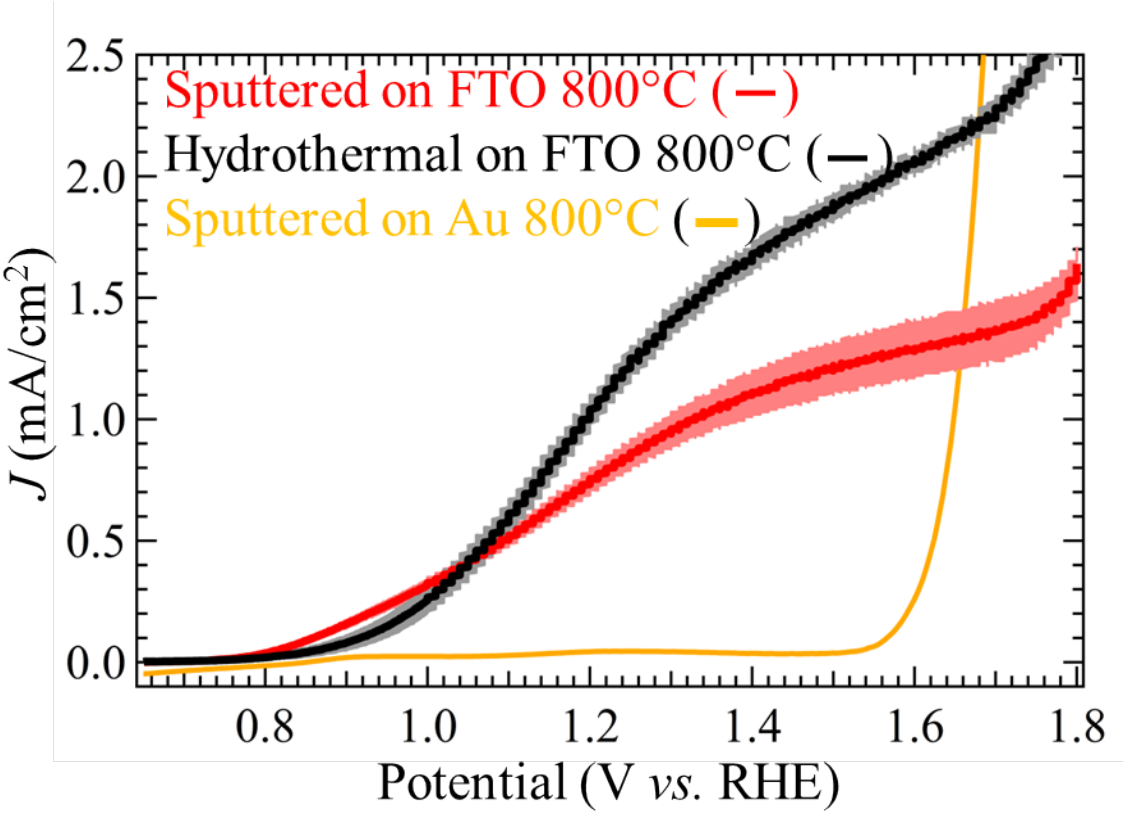

Figure S2. (a) (Top) Optical image of the sputtered α-Fe_2O_3 samples of thickness 600 nm at room temperature, after annealing at 500 °C for 2 h, and after annealing at 800 °C for a further 10 min. (Bottom) Hydrothermal samples of thickness 300 nm at room temperature, after annealing at 500 °C for 2 h, and after annealing at 800 °C for a further 10 min. The yellow FeOOH in the room temperature sample contrasts with the red α-Fe_2O_3 of the annealed samples. (b) Optical image of sputtered and hydrothermal samples after annealing at 800 °C illuminated from the back; the non-uniform coverage of the hydrothermal sample is apparent. Each slide has dimensions of 25 mm × 25 mm. Scanning electron microscope image of the top of sputtered (c) and hydrothermal (d) α-Fe_2O_3 samples annealed at 500 °C for 2 h, followed by 800 °C for 10 min. The larger surface area of the hydrothermal samples in (d) is apparent.

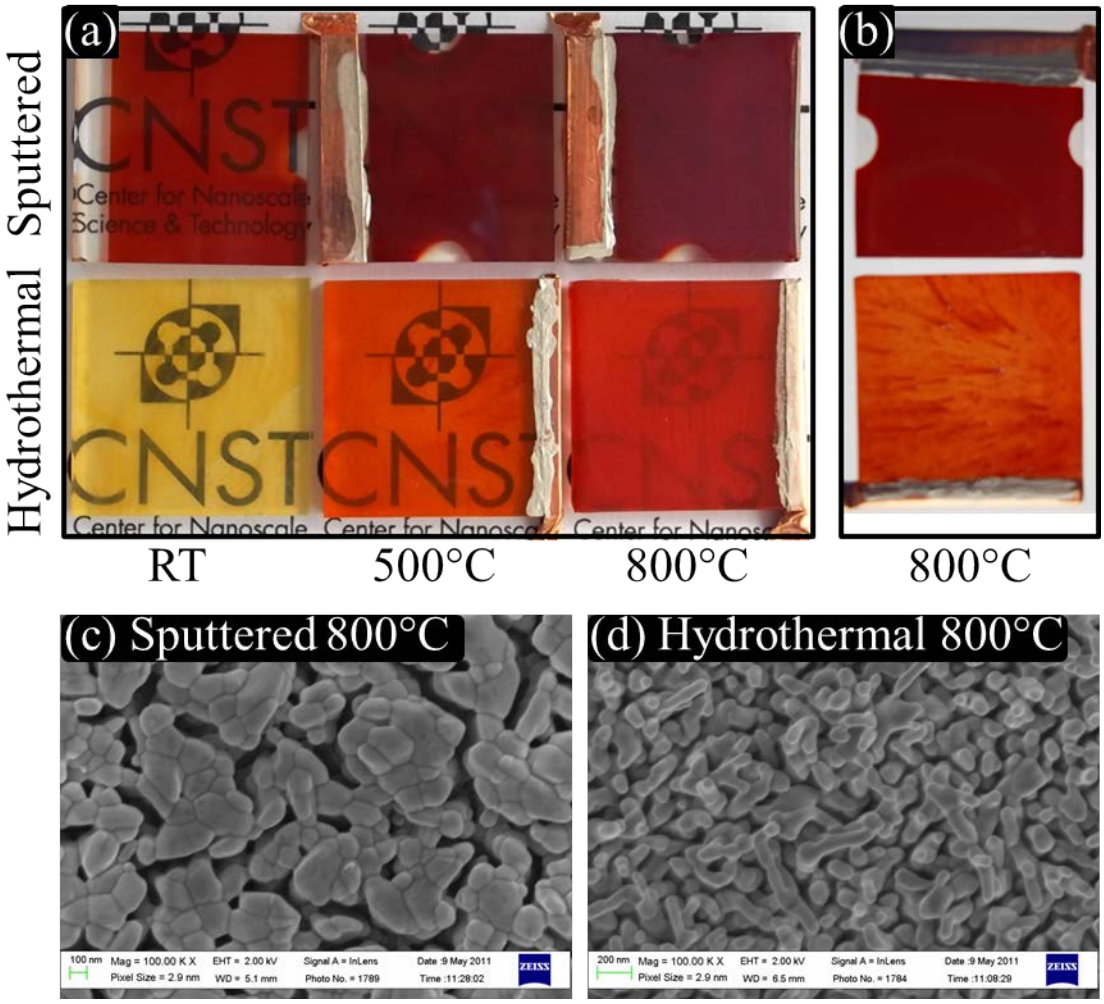

Figure S3. Absorbance versus wavelength (λ) or energy (*E*) of α-Fe_2O_3 sputtered samples of thickness 600 nm on FTO, hydrothermal samples of thickness 300 nm on FTO and blank FTO of thickness 600 nm at room temperature (blue), after annealing at 500 °C for 2 h (black), and after further annealing at 800 °C for 10 min (red). The cut-on absorbance shifts towards higher wavelengths upon heat treatment for the sputtered and hydrothermal samples. Incomplete coverage of the α-Fe_2O_3 in the hydrothermal samples is apparent as two absorbance regions corresponding to α-Fe_2O_3 and FTO are distinguishable, indicated by down arrows. Shading indicates a single standard deviation calculated from at least three experiments.

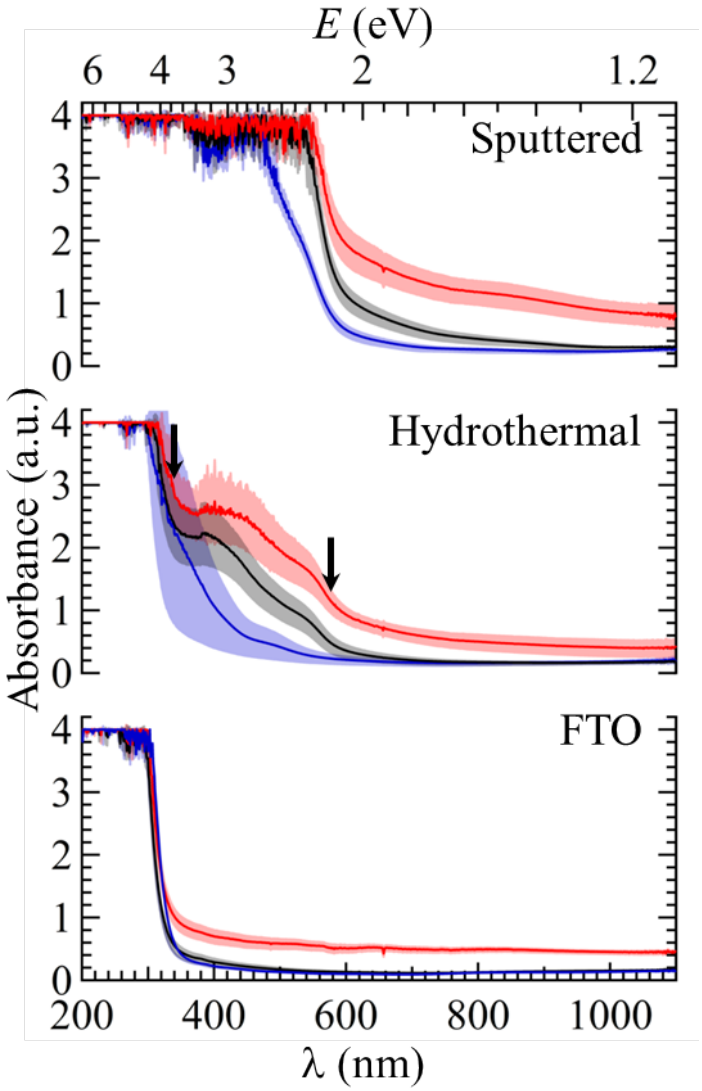

Figure S4. X-ray diffraction patterns in order from bottom to top of eight samples: amorphous soda lime float glass; amorphous soda lime float glass coated with 600 nm FTO; as deposited hydrothermal samples on FTO; hydrothermal samples on FTO heated to 500 °C for 2 h; hydrothermal samples on FTO heated to 500 °C for 2 h followed by 800 °C for 10 min; sputtered α -Fe_2O_3 on FTO; sputtered α -Fe_2O_3 on FTO heated to 500 °C for 2 h; sputtered α -Fe_2O_3 on FTO heated to 500 °C for 2 h followed by 800 °C for 10 min. The thicknesses of the sputtered and hydrothermal samples are 600 nm and 300 nm, respectively.

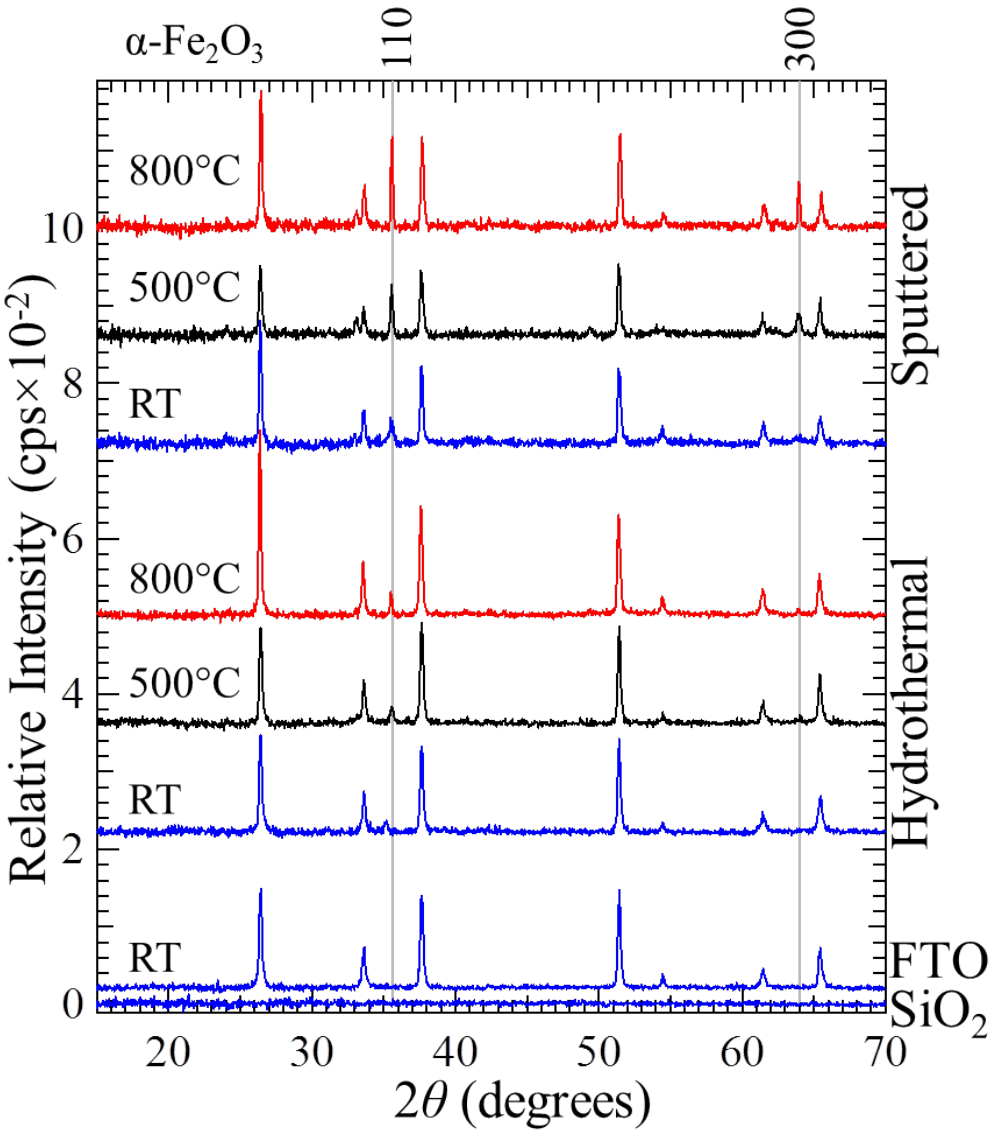

Figure S5. Mott-Schottky plots of the square of the inverse capacitance *vs*. potential for the blank FTO substrate at three different frequencies: 10^2 Hz (blue), 10^3 Hz (black) and 10^4 Hz (red). The electrolyte was 1 mol/L NaOH (pH 13.6); experiments were conducted in the dark; the samples had been annealed at 500 °C for 2 h (a), followed by 800 °C for 10 min (b). Shading indicates a single standard deviation calculated from at least three experiments.